J Mater Sci: Mater Med (2011) 22:2311–2318
DOI 10.1007/s10856-011-4406-4

Hemocompatibility investigation of the NiTi alloy implanted with tantalum

Tingting Zhao · Yan Li · Yuzhi Gao · Yan Xiang · Hong Chen · Tao Zhang

Received: 17 March 2011 / Accepted: 28 July 2011 / Published online: 11 August 2011

Abstract A composite TiO_2/Ta_2O_5 nano-film has been formed on the NiTi shape memory alloy by Ta implantation. The wettability, protein adsorption, platelets adhesion and hemolysis tests are conducted to evaluate the hemocompatibility. The contact angle measurements showed that the surface of the NiTi alloy kept hydrophilic before and after Ta implantation, although the water contact angle increased with the increasing of implantation current. Both of the surface energy and the interfacial tension decreased after Ta implantation. The protein adsorption behavior was investigated by ^{125}I isotope labeling. The fibrinogen adsorption was enhanced by a high surface roughness or a large interfacial tension, while the albumin adsorption was insensitive to the surface modification. Platelet adhesion and activation were weakened and the hemolysis rate was reduced at least 46% after Ta implantation due to the decreased surface energy and improved corrosion resistance ability, respectively.

T. Zhao · Y. Li (✉) · Y. Gao
School of Materials Science and Engineering,
Beihang University, #37, Xueyuan Road,
Beijing 100191, People's Republic of China
e-mail: liyan@buaa.edu.cn

T. Zhao · Y. Li
Key Laboratory of Aerospace Materials and Performance
(Ministry of Education), Beihang University,
Beijing 100191, People's Republic of China

Y. Xiang
School of Chemistry and Environment, Beihang University,
Beijing 100191, People's Republic of China

H. Chen
School of Materials Science and Engineering,
Wuhan University of Technology, Wuhan 430070, China

T. Zhang
Key Laboratory of Beam Technology and Material Modification
of Ministry of Education, Beijing Normal University,
Beijing 100875, China

1 Introduction

The conventional metals or alloys used in stent construction are stainless steel, CoCr alloys, tantalum and Nitinol (NiTi). NiTi alloys are superior materials candidates in the application of self-expanding stents, owing to their unique shape memory properties and excellent corrosion resistance [1–3]. However, these alloys are questioned about their hemocompatibility as the blood-contacting materials. Comparing with the other conventional stent materials, stainless steel and cp-Ti, NiTi alloy was reported to significantly reduce thrombogenicity [4, 5] but increased platelets adhesion [6, 7]. Apparently, the application of NiTi alloys in blood contacting implants requires better hemocompatibility. As most of blood-biomaterials interactions take place at the surface of the implant, surface modification of NiTi alloys to improve hemocompatibility has become the focus of the research.

A broad spectrum of surface modification methods has shown great potential for improving the hemocompatibility of NiTi alloy. Plasma based ion implantation was used to deposit diamond-like carbon (DLC) films on NiTi alloys, and the DLC coated NiTi alloy showed lower amount of platelets adhered and no tendency of platelets aggregation compared with that of non-treated NiTi alloy [8]. Oxidation treatment (oxidized at 400°C and 3×10^{-2} mbar for 2 h 30 min) created a Ni-free surface, enhanced the hydrophilic character of NiTi alloy and increased the amount of fibronectin and albumin adsorbed [9]. Cathodic electrophoretic deposition of chitosan-heparin films on NiTi alloy

was reported to bind much greater antithrombin, suggesting improved hemocompatibility as well [10]. Ion implantation is another versatile strategy [11] which modifies the surface of NiTi without altering the shape memory and pseudoelastic properties of bulk alloys. Ion implantation of C [12], O [13] or Mo + C [14] into NiTi alloy was reported to modify the surface morphology, chemical composition and to increase oxide layer thickness. All those modified surface characteristics would in turn influence the cell behavior on NiTi alloy. For instance, the adhesion and proliferation of osteoblasts were enhanced on C or O implanted NiTi, owing to the suppressed Ni surface concentration [12, 13]. Prolonged dynamic clotting time and decreased hemolysis, indicating a better hemocompatibility, were reported on Mo + C ion implantation modified NiTi alloy [14].

Our group attempted to modify NiTi using metal ions Ta implantation for its excellent corrosion resistance and biocompatibility properties. We have demonstrated that a TiO_2–Ta_2O_5 composite surface layer formed on NiTi alloy after Ta implantation [15, 16]. This layer of TiO_2–Ta_2O_5 was proved to improve the corrosion resistance of NiTi alloy and favor the adhesion and proliferation of both smooth muscle cell and osteoblasts [17]. However, the hemocompatibility of NiTi modified by Ta implantation is yet a question. The relation between the surface characteristics and the hemocompatilibty of biomaterials is not well understood [18]. Hence, in the present work, the hemocompatibility of Ta-implanted NiTi was investigated in the aspects of protein adsorption, platelets adhesion and hemolysis. The observations were further discussed based on the surface characteristic analysis of the wettability, surface energy, interfacial tension, surface roughness and surface chemistry.

2 Materials and methods

2.1 Specimens preparation

NiTi alloy plate with 50.6 at% Ni (Beijing GEE Technology & Trade Company, China) was cut into samples of $8 \times 8 \times 1$ mm^3. The specimens were sealed in vacuum quartz ampoules that were then annealed at 873 K for 30 min followed by water quenching. The NiTi alloy is in the austenite phase at room temperature (298 K) because of its lower martensitic transformation temperatures as seen in Ref. [15]. The NiTi plates then underwent progressive wet grinding with 280–2,000 grits SiC emery papers, polished to a mirror surface texture with diamond paste (3.5 μm finish), and cleaned ultrasonically with acetone, anhydrous ethanol and distilled water for 10 min in each prior to implantation. The Ta implantation process was carried out using metal vapor vacuum arc plasma source (MEVVA 100). The implantation parameters are displayed in Table 1, which are identical with those in Ref. [16]. Before ion implantation, samples were sputtered with energetic argon ions at −5 kV to remove any residual surface contaminants. The implanted target material was pure Ta (99.99%; General Research Institute for Nonferrous Metals, China). All of the samples were cleaned ultrasonically again after Ta implantation.

Table 1 Implantation parameters

Sample	NiTi	1 mA NiTi	2 mA NiTi	4 mA NiTi
Ion current (mA)	0	1	2	4
Dose ($\times 10^{17}$ ions/cm^2)	0	1.0	1.0	1.0
Base pressure (Pa)	0	1×10^{-4}	1×10^{-4}	1×10^{-4}
Bias voltage (kV)	0	−45	−45	−45

2.2 Contact angles

Contact angles were measured using the liquid drop method on a contact angle goniometer (HARKE, China) at 298 K. Two different liquids were used to carry out the measurements: ultrapure water and glycol. A 5 μl droplet of the liquid was dropped on the surface of the sample, and an image of the droplet was captured immediately after stabilization and every 5 s. The profile of the droplet was automatically fitted and analyzed with the software supplied by the manufacturer. At least three samples were measured in each group, and two different points were chosen on each sample. The final values were given as the means ± SD.

2.3 Surface energy and interfacial tension calculation

Surface energy can be determined by contact angle. The values of the polar and dispersive components of ultrapure water and glycol are shown in Table 2. The surface free energies (SFE) of the samples were calculated using the Owens and Wendt model, which gives the long-range dispersion (Lifshitz–van der Waals) (γ^d) and the short-range polar (hydrogen bonding) (γ^p) components of surface free energy [20]. For this method, the spreading pressure

Table 2 Values of the polar, γ^p, and dispersive, γ^d, components of the surface energy of ultrapure water and glycol [19]

Liquid	Dispersive component (γ^d, mJ/m^2)	Polar component (γ^p, mJ/m^2)
Ultrapure water	21.8	51.0
Glycol	29.3	19.0

was not taken into account for the SFE values are lower than 60 mJ/m^2 [21] in the present study. Both polar, γ^{p}, and dispersive, γ^{d}, components of the SFE of each sample surface can be obtained according to the following equations:

$$\gamma_L(1+\cos\theta) = 2\left((\gamma_L^d\gamma_S^d)^{1/2} + (\gamma_L^p\gamma_S^p)^{1/2}\right) \quad (1)$$

where γ_{L} and γ_{S} are related to the liquid surface energy and solid surface energy, respectively.

Interfacial tension can be obtained using the $\gamma_{\mathrm{s}}^{\mathrm{p}}$ and $\gamma_{\mathrm{s}}^{\mathrm{d}}$ of the SFE. The values of the surface tension of blood components are shown in Table 3. The interfacial tension between the surface of the sample and blood components can be calculated from the formula (2):

$$\gamma_{\mathrm{sbc}} = \left[\left(\gamma_{bc}^p\right)^{1/2} - \left(\gamma_s^p\right)^{1/2}\right]^2 + \left[\left(\gamma_{bc}^d\right)^{1/2} - \left(\gamma_s^d\right)^{1/2}\right]^2 \quad (2)$$

where γ_{sbc} is the interface tension between solid and blood components; $\gamma_{\mathrm{bc}}^{\mathrm{p}}$ and $\gamma_{\mathrm{bc}}^{\mathrm{d}}$ are the polar and dispersion surface tension of blood components, respectively.

2.4 Protein adsorption

Two different proteins were used for the adsorption assay: fibrinogen (Calbiochem) and human serum albumin (HSA; Sigma). Proteins were labeled with ^{125}I (Isotope company of China, Beijing) using the iodine monochloride (ICl) method [22]. Unincorporated ^{125}I was separated from the labeled protein by passing through AG-1-X4 resin column (Bio-Rad Laboratories, Hercules, CA). The concentration of ^{125}I-fibrinogen was determined spectrophotometrically by measuring the absorption at 280 nm using an ultraviolet spectrophotometer (GBC Cintra 10e; Australia). This solution was stored at 203 K and used within the next 2 weeks.

All of the samples were ultrasonically cleaned with acetone, anhydrous ethanol and distilled water for 10 min, respectively, prior to test. For studies of protein adsorption from buffer, labeled and unlabeled proteins (1:19, labeled: unlabeled) were mixed at a total concentration of 1 mg/ml. Each of the untreated and Ta modified NiTi samples was placed into wells of 48-well tissue culture plate and 500 μl TBS was added separately for 2 h to achieve equilibrium. Then the samples were incubated with proteins in buffer for 2 h at 298 K. After the incubation process, the samples were rinsed three times, 10 min each with TBS, wicked onto filter paper, and transferred to clean tubes for radioactivity determination by gamma counter (Perkin–Elmer Life Sciences, USA). The radioactivity was converted to adsorbed protein amount. The results expressed were obtained by taking into account the instrument background and expressed as microgram per square centimeter (μg/cm^2). Two independent experiments were performed to ensure reproducibility of the results.

Table 3 Surface tension of blood components [19]

Blood components	Dispersive component (γ^{d}, mJ/m^2)	Polar component (γ^{p}, mJ/m^2)	Surface energy (γ, mJ/m2)
Blood	11.2	36.3	47.5
Fibrinogen	24.7	40.3	65.0
Albumin	31.4	33.6	65.0

2.5 Blood platelet adhesion test

In vitro platelet adhesion test was performed, utilizing fresh human blood, to evaluate the thrombosis resistant property of the untreated and modified NiTi alloys. ACD, a kind of anticoagulant including citrate acid and citrate sodium and dextrose, was added into the fresh human blood with a blood to ACD ratio of 10:1. The solution was centrifuged at $200\times g$ for 10 min to get platelet-rich plasma (PRP). Untreated and modified NiTi alloys (three parallel samples for each) were put into a 24-well tissue culture plate, and 0.5 ml aliquot of the PRP was added to each well. After incubation at 310 K for 1 h, the samples were taken out from the wells and rinsed with phosphate-buffered solution (PBS) for three times to get rid of the loosely adsorbed platelets. The samples were then soaked in 2.5% glutaraldehyde at room temperature for 1 h to fix the adhered platelets. After washing with PBS, the platelets were subsequently dehydrated in 30, 50, 70, 90 and 100% ethanol for twice at each step and 15 min per time. Then the samples were allowed to dry naturally, and coated with thin films of gold in order to observe the distribution and morphology of the adhered platelets. To count the platelets number, ten different areas were chosen and platelets were counted by plugins of Image J software (developed by the National Institutes of Health) [23].

2.6 Hemolysis

8 ml fresh anticoagulant human being blood (10:1, blood:ACD) was diluted with 10 ml 0.9% saline. Each test sample was immersed into 10 ml saline and incubated at 310 K for 30 min. Afterwards, 0.2 ml diluted blood was added into the saline, mixed uniformly and maintained for another 60 min. After incubation, the suspension was centrifuged at 2,500 rpm for 5 min. The absorbance of the supernatant solution was measured by a UV–visible spectrophotometer (GBC Cintra 10e, Australia) at wavelength of 545 nm. A mixture of blood and deionized water was used as the positive control and a mixture of blood and saline was used as the negative control. The hemolysis rate was calculated from the formula (3):

$$A(\%) = (D_t - D_{nc})/(D_{pc} - D_{nc}) \quad (3)$$

Where A represents hemolysis rate; D_t, D_{nc} and D_{pc} mean the adsorbance of the samples, the negative control and the positive control respectively. The hemolysis rate for each sample was mean values of three measurements.

2.7 Data analysis

Three different specimens ($N = 3$) were used in each study and statistical evaluation of the data was performed using Student's t test. The probability (P) values of less than 0.05 ($P < 0.05$) were considered to be statistically significant differences.

3 Results and discussion

3.1 Contact angle and surface energy

Water contact angles and surface energies of the untreated and Ta-implanted NiTi samples are shown in Fig. 1. The water contact angle of the untreated NiTi sample was 53.9°. For 1 mA NiTi, the water contact angle was 54.1°, which is very close to that of the untreated NiTi. With the increase of incident current from 1 to 4 mA, the water contact angle of the Ta-implanted NiTi samples increased significantly from 54.1° to 64.0°. With the similar trend, the total surface energy of 1 mA NiTi sample did not alter effectively. However, with the increase of current from 1 mA to 4 mA, the total surface energy of Ta-implanted NiTi sample became lower than that of the untreated NiTi sample. The polar component of surface energy γ^p and dispersive component of surface energy γ^d were measured as 45.0 and 4.1 mJ/m^2 for the untreated NiTi sample, respectively. The γ^p decreased significantly after Ta implantation at 2 and 4 mA, in contrast with γ^d. The γ^p accounted for the larger part in surface energy for all the samples and the ratio of γ^p/γ decreased with the increasing incident current from 0.92 of the untreated NiTi to 0.62 of 4 mA NiTi sample, respectively.

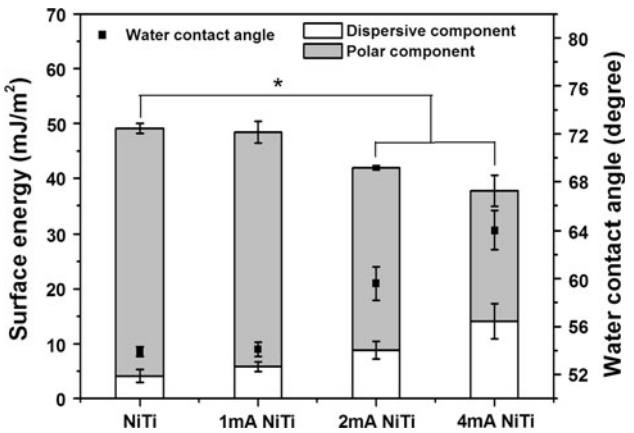

Fig. 1 Water contact angle and surface energy of the untreated and Ta-implanted NiTi samples (*$P < 0.05$, mean ± SD, $N = 3$)

The results of water contact angle measurement and surface energy calculation indicated that NiTi became less hydrophilic after Ta implantation, but was still below the theoretical limit of 65° between hydrophilic and hydrophobic characters [24]. It is believed that the increase of relative hydrophobicity for the Ta-implanted NiTi with the increasing implantation current originated from the decrease of γ^p/γ. The polar component attracts the electric dipoles of water leading to minimum interfacial energy and lower water contact angle [25]. Palmaz [26] showed that metals may cause thrombogenicity due to its high surface free energy. And Chen [18] has demonstrated that lower surface energy enhanced hemocompatibility of Ti (Ta^{+5}) O_2 thin films. Therefore, the decrease of surface energy of Ta-implanted NiTi observed in this study may be an advantage for the improvement of anti-thrombus ability.

3.2 Interfacial tension

The interfacial tension (γ_{sbc}) values between the untreated and Ta-implanted NiTi sample surfaces with water, blood, fibrinogen and albumin are listed in Table 4. In comparison to interfacial tension values of untreated NiTi alloy, each interfacial tension value of the Ta implanted NiTi alloy was reduced in spite of the type of biological substance. Among all the Ta-implanted NiTi samples, the 2 mA NiTi sample exhibited the lowest interfacial tension value in the case of water, blood and fibrinogen.

It is known that high interfacial tension could enable proteins to anchor and adhere strongly onto surface [27], leading to the denaturation of adsorbed protein and the initiation of further coagulation cascade. For instance, it has been proved that titanium oxide films had better hemocompatibility due to its lower interfacial tension comparing with the low temperature isotropic pyrolytic carbon (LTIC) [19]. The interfacial tension of the Ta-implanted NiTi with biological substances was lower

Table 4 Interfacial tension (γ_{sbc}) between the untreated and Ta-implanted NiTi sample surfaces with biological substances

Biological substances	NiTi	1 mA NiTi	2 mA NiTi	4 mA NiTi
Water	7.5	5.7	4.3	5.9
Blood	2.7	1.3	0.2	1.4
Fibrinogen	9.4	6.9	3.2	3.6
Albumin	14.5	11.2	5.0	4.3

than that of the untreated NiTi sample as seen in Table 4. Thus, it is conceivable that the lower interfacial tension of the Ta-implanted NiTi could be beneficial for less protein adsorption and distortion, and hence could improve the hemocompatibility.

3.3 Protein adsorption

The amount of proteins (fibrinogen and albumin) adsorbed on the untreated and Ta-implanted NiTi and the roughness of each sample are presented in Fig. 2. The fibrinogen adsorption on the untreated NiTi was significantly higher than that on 1 and 4 mA Ta-implanted NiTi, but was similar to that on 2 mA NiTi. For albumin adsorption, the three Ta-implanted NiTi did not show any statistically significant difference comparing with untreated NiTi. It was also found that the fibrinogen adsorption was higher than the albumin adsorption regardless of substrate surface condition, which is consistent with the finding of Cai et al. [27]. It is also worth noting that the surface roughness was altered due to Ta implantation and its maximum was 13.89 nm observed on the 2 mA NiTi [16].

Interaction between a biomaterial and blood starts with the adsorption of plasma proteins onto material surface within a few seconds leading to the formation of a protein adsorption layer (10–20 nm). The category and quantity of proteins that are firstly adsorbed on the surface will influence the subsequent coagulation process. Adsorption of fibrinogen is believed to induce thrombus formation by directly participating in the coagulation cascade or through promoting platelet adhesion and activation, while adsorption of albumin may prolong the coagulation time by decreasing adhesion and activation of platelet. Thus, for better hemocompatibility, the surface of a biomaterial needs to absorb more albumin rather than fibrinogen. As shown in Fig. 2, the fibrinogen absorbed on NiTi was

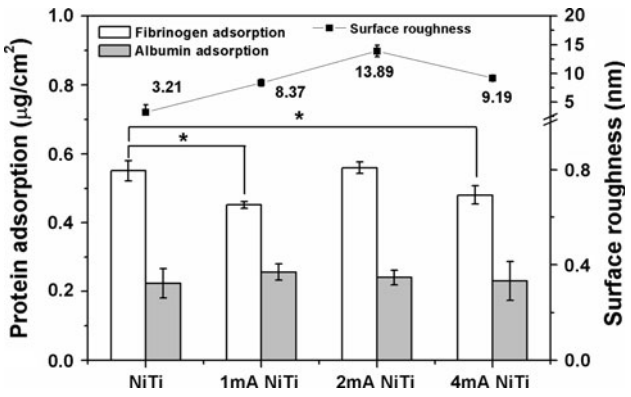

Fig. 2 The amount of adsorbed proteins (fibrinogen and albumin) and the surface roughness of the untreated and Ta-implanted NiTi samples ($^*P < 0.05$, mean ± SD, $N = 3$). The data of the surface roughness is cited from Ref. [16]

obviously reduced after Ta implantation except for the 2 mA NiTi. We believe that both of the roughness and interfacial tension contributed to the fibrinogen absorption behavior in Fig. 2. A higher roughness led to more fibrinogen adsorption as seen in Fig. 2, which was partly supported by the fact that the amount of fibrinogen adsorption on tantalum films was increased with the increasing roughness from 2 to 32.9 nm [28]. Simultaneously, a lower fibrinogen-surface interfacial tension tended to absorb less fibrinogen on the surface. No considerable difference can be found among all the samples for albumin adsorption. This may be because that the albumin adsorption on NiTi alloy is essentially insensitive to the surface roughness and interfacial tension as can be seen in the NiTi [29] and the oxygen-implanted NiTi [30].

3.4 Blood platelet adhesion

The SEM morphologies of the platelets adhered on the surface of the untreated and Ta-implanted NiTi samples after 1 h incubation are shown in Fig. 3. It is seen from Fig. 3a that the platelets on the surface of untreated NiTi sample were activated seriously with pseudopodia spread on the surface. Most of the platelets were spread dendritic (SD) shapes and some were in fully spread shapes (FS) [31], suggesting serious propensity for thrombosis. For the Ta-implanted NiTi samples, most of the platelets were slightly activated with dendritic (D) shapes, as shown in Fig. 3b, c, d. In addition, no obvious accumulations of platelets were observed on all the samples. The statistical results of the platelet adhesion after 1 h incubation are estimated in Fig. 4. It was found that untreated NiTi sample had the largest amount of platelets, while the 4 mA NiTi sample had the least platelet number. The platelet number on Ta-implanted NiTi decreased with the increasing of incident current.

Platelet adhesion and activation onto the surface of biomaterials, which have been linked to the formation of thrombogenicity, are the most essential characteristics in determining the hemocompatibility [25]. It has been indicated that the platelet activation was the result of differences in surface chemistry [7]. As our results have shown, TiO_2–Ta_2O_5 composite surface layer on Ta-implanted NiTi has an advantage over the TiO_2 surface layer on the untreated NiTi in platelet adhesion and activation. This is supported by the study of Timothy [32] that the untreated NiTi was proved to be thrombogenic despite its hydrophilic surface. Furthermore, the platelet number on the Ta-implanted NiTi decreased with the increasing of incident current as seen in Fig. 4. This was attributed to the surface energy rather than the surface roughness, since the nano-scale surface roughness was too small to influence the platelet with 3 μm in diameter in their resting state [33]. Comparing Fig. 1 with 4, a positive correlation was established between the number

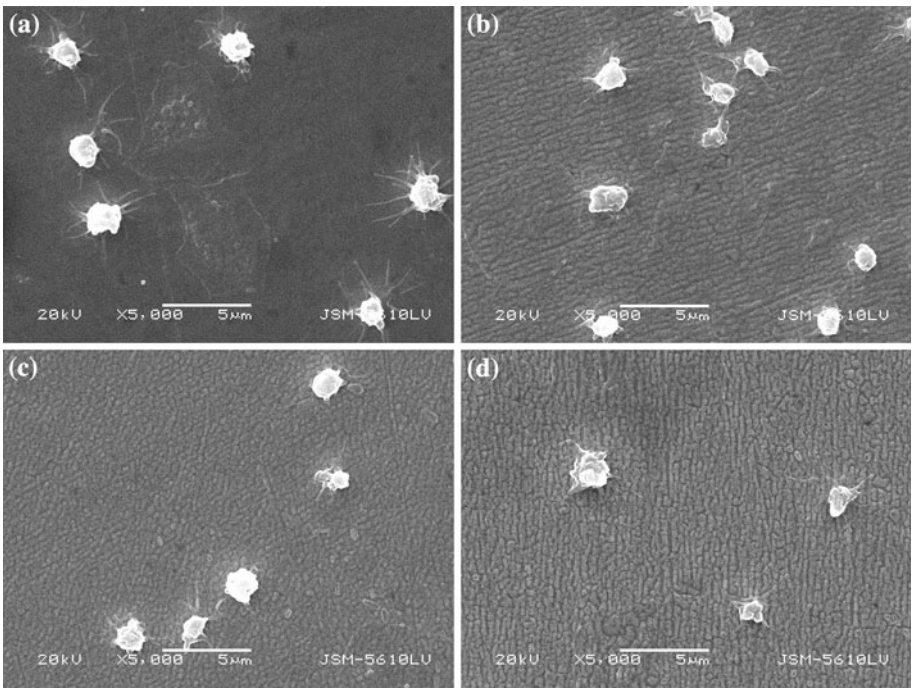

Fig. 3 Morphologies of adherent platelets on the surface of **a** NiTi, **b** 1 mA NiTi, **c** 2 mA NiTi and **d** 4 mA NiTi samples after 1 h incubation in PRP

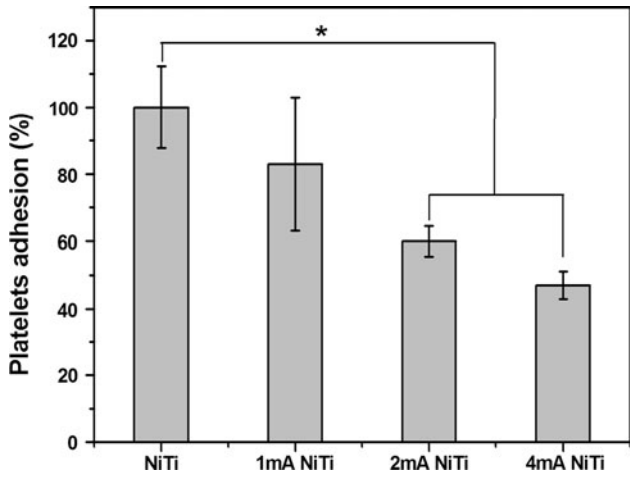

Fig. 4 The number of platelets adhered on the untreated and Ta-implanted NiTi samples in contact with PRP for 1 h ($*P < 0.05$, mean ± SD, $N = 3$). The average number and standard deviation of adherent platelets on the modified NiTi substrate are displayed as those on the control substrate (100%)

of platelets adhered and the surface energy (or γ^p/γ) of the Ta-implanted NiTi. Therefore, it is concluded that a lower surface energy (or γ^p/γ) was beneficial to the hemocompatibility, which was consistent with the study on Ti $(Ta^{+5})O_2$ thin films [18].

3.5 Hemolysis

The hemolysis rates of the untreated and Ta-implanted NiTi samples are listed in Table 5. The hemolysis rate of the untreated NiTi was 0.681, which was comparable to the value of 0.4306 reported in literature [14], however, the hemolysis rate was decreased by at least 46% after Ta implantation. A lower hemolysis rate indicated less hemolysis occurring on the surface. Hence, we could conclude that Ta implantation improved the hemolysis resistance of NiTi surface. In addition, the hemolysis rates of all the NiTi samples reported in this study was in the range of 0.26–0.68%, which was much less than the hemolytic level of 5%, indicating that none of the samples had significant hemolytic effect.

Hemolysis in contact with biomaterials or their extraction products is a significant screening method used in hematology. The breakdown of erythrocytes directly impairs the ability of the circulatory system to transport oxygen to the body's tissues. As shown in Table 5, the Ta-implanted NiTi samples performed better than the untreated NiTi on hemolysis. The hemolysis rate of 1 mA NiTi and 2 mA NiTi samples is 0.268 and 0.262, respectively, which are slightly lower than that of C-implanted NiTi (0.2871) [14]. It appeared that the reason for the

Table 5 Hemolysis rate of untreated and Ta-implanted NiTi sample surfaces

	NiTi	1 mA NiTi	2 mA NiTi	4 mA NiTi
Hemolysis rate (%)	0.681 ± 0.001	0.268 ± 0.002	0.262 ± 0.001	0.366 ± 0.003

improved hemolytic behavior of Ta-implanted NiTi could be ascribed to the improvement of the corrosion resistance after Ta implantation [15, 16], which decreased the concentration of dissolved toxic substance and thus reduced the damage to erythrocyte. In addition, semiconducting behavior of $Ti(Ta^{+5})O_2$ oxide layer with optical bandgap of 3.2 eV [18], which is n-type semiconductor in nature, helps to prevent proteins on the material surface from denaturing by preventing charge transfer from protein into the material, which is correlated with the formation of thrombus on an artificial material [34].

4 Conclusions

A composite TiO_2/Ta_2O_5 nano-film has been formed on the NiTi shape memory alloy by Ta implantation. The results showed that the surface of the NiTi alloy was hydrophilic and the water contact angle increases with the increasing of implantation current. Both of the surface energy and the interfacial tension decreased after Ta implantation. A high surface roughness or a large interfacial tension was beneficial to the fibrinogen adsorption, but no difference was displayed for the albumin adsorption among different samples. Platelet adhesion and activation were weakened and the hemolysis rate was decreased by at least 46% after Ta implantation due to the decreased surface energy and improved corrosion resistance ability, respectively. Ta implantation technique is an effective method to improve the hemocompatibility of NiTi biomedical alloys.

Acknowledgments This work is supported by National Natural Science Foundation of China (NSFC), No. 50971007 and the Innovation Foundation of BUAA for PhD Graduates. Yan Li acknowledges the funding by the Program for New Century Excellent Talents in University (NCET-09-0024).

References

1. Shabalovskaya A. Surface, corrosion and biocompatibility aspects of Nitinol as an implant material. Bio-Med Mater Eng. 2002;12:69–109.
2. McKenna CJ, Holmes DR, Schwartz RS. Novel stents for the prevention of restenosis. Trends Cardiovasc Med. 1997;7:245–9.
3. Machado LG, Savi MA. Medical applications of shape memory alloys. Braz J Med Biol Res. 2003;36:683–91.
4. Thierry B, Merhi Y, Bilodeau L, Trepanier C, Tabrizian M. Nitinol versus stainless steel stents: acute thrombogenicity study in an ex vivo porcine model. Biomaterials. 2002;23:2997–3005.
5. Bai ZJ, Filiaggi MJ, Dahn JR. Fibrinogen adsorption onto 316L stainless steel, Nitinol and titanium. Surf Sci. 2009;603:839–46.
6. Plant SD, Grant DM, Leach L. Surface modification of NiTi alloy and human platelet activation under static and flow conditions. Mater Lett. 2007;61:2864–7.
7. Armitage DA, Parker TL, Grant DM. Biocompatibility and hemocompatibility of surface-modified NiTi alloys. J Biomed Mater Res. 2003;66A:129–37.
8. Cheng Y, Zheng YF. The corrosion behavior and hemocompatibility of TiNi alloys coated with DLC by plasma based ion implantation. Surf Coat Technol. 2006;200:4543–8.
9. Michiardi A, Aparicio C, Ratner BD, Planell JA, Gil J. The influence of surface energy on competitive protein adsorption on oxidized NiTi surfaces. Biomaterials. 2007;28:586–94.
10. Sun F, Sask KN, Brash JL, Zhitomirsky I. Surface modifications of Nitinol for biomedical applications. Colloids Surf B. 2008; 67:132–9.
11. Anders André, et al. Handbook of plasma immersion ion implantation and deposition. New York: Wiley; 2000.
12. Poon RWY, Yeung KWK, Liu XY, Chua PK, Chung CY, Lu WW, et al. Carbon plasma immersion ion implantation of nickel–titanium shape memory alloys. Biomaterials. 2005;26:2265–72.
13. Yeung KWK, Poon RWY, Liu XY, Ho JPY, Chung CY, Chu PK, et al. Investigation of nickel suppression and cytocompatibility of surface-treated nickel-titanium shape memory alloys by using plasma immersion ion implantation. J Biomed Mater Res A. 2005; 72(3):238–45.
14. Liang CH, Huang NB. Study on hemocompatibility and corrosion behavior of ion implanted TiNi shape memory alloy and Co-based alloys. J Biomed Mater Res A. 2007;83:235–40.
15. Li Y, Wei SB, Cheng XQ, Zhang T, Cheng GA. Corrosion behavior and surface characterization of tantalum implanted TiNi alloy. Surf Coat Technol. 2008;202:3017–22.
16. Li Y, Zhao TT, Wei SB, Xiang Y, Chen H. Effect of Ta_2O_5/TiO_2 thin film on mechanical properties, corrosion and cell behavior of the NiTi alloy implanted with tantalum. Mater Sci Eng C. 2010;30:1228–36.
17. Zhao TT, Yang RX, Zhong C, Li Y, Xiang Y. Effective inhibition of nickel release by tantalum-implanted TiNi alloy and its cytocompatibility evaluation in vitro. J Mater Sci. 2011;46:2529–35.
18. Chen JY, Leng YX, Tian XB, Wang LP, Huang N, Chu PK, Yang P. Antithrombogenic investigation of surface energy and optical bandgap and hemocompatibility mechanism of $Ti(Ta^{+5})O_2$ thin films. Biomaterials. 2002;23:2545–52.
19. Huang N, Yang P, Leng YX, Chen JY, Sun H, Wang J, Wang GJ, Ding PD, Xi TF, Leng Y. Hemocompatibility of titanium oxide films. Biomaterials. 2003;24:2177–87.
20. Ponsonnet L, Reybier K, Jaffrezic N, Comte V, Lagneau C, Lissac M, Martelet C. Relationship between surface properties (roughness, wettability) of titanium and titanium alloys and cell behaviour. Mater Sci Eng C. 2003;23(4):551–60.
21. Busscher HJ. Wettability of surfaces in the oral cavity. In: Schrader ME, Loeb GI, editors. Modern approaches to wettability. New York: Plenum; 1992. p. 249–61.
22. Chen H, Zhang Z, Chen Y, Brook MA, Sheardown H. Protein repellant silicone surfaces by covalent immobilization of poly(ethylene oxide). Biomaterials. 2005;26:2391–9.
23. National Institutes of Health. In: Image J home. http://rsb.info.nih.gov/ij/download.html.
24. Shibuichi S, Onda T, Satoh N, Tsujii K. Super water-repellent surfaces resulting from fractal structure. J Phys Chem. 1996; 100:19512–7.
25. Roy RK, Choi HW, Yi JW, Moon MW, Lee KR, Han DK, Shin JH, Kamijo A, Hasebe T. Hemocompatibility of surface-modified, silicon-incorporated, diamond-like carbon films. Acta Biomater. 2009;5:249–56.
26. Palmaz JC. Intravascular stents: tissue-stent interaction and design consideration. AJR Am J Roentgenol. 1993;160:613–8.
27. Cai KY, Bossert J, Jandt KD. Does the nanometre scale topography of titanium influence protein adsorption and cell proliferation? Colloids Surf B. 2006;49:136–44.
28. Rechendorff K, Hovgaard MB, Foss M, Zhdanov VP, Besenbacher F. Enhancement of protein adsorption induced by surface roughness. Langmuir. 2006;22:10885–8.

29. Clarke B, Kingshott P, Hou X, Rochev Y, Gorelov A, Carroll W. Effect of Nitinol wire surface properties on albumin adsorption. Acta Biomater. 2007;3:103–11.
30. Tan L, Bauer J, Crone WC, Albrecht RM. Biocompatibility improvement of NiTi with a functionally graded surface. In: Proceedings of the SEM annual conference on experimental mechanics, Milwaukee; 2002. p. 131–4.
31. Goodman SL. Sheep, pig, and human platelet–material interactions with model cardiovascular biomaterials. J Biomed Mater Res. 1999;42:240–50.
32. McPherson TB, Shim HS, Park K. Grafting of PEO to glass, Nitinol, and pyrolytic carbon surfaces by γ irradiation. J Biomed Mater Res. 1997;38:289–302.
33. Shabalovskaya S, Anderegg J, Humbeeck JV. Critical overview of Nitinol surfaces and their modifications for medical applications. Acta Biomater. 2008;4:447–67.
34. Sunny MC, Sharma CP. Titanium–protein interaction: change with oxide layer thickness. J Biomater Appl. 1991;5(6):89–98.